Influence of detailed line treatment on the opacity of iron plasmas in the 2*p*-3*d* energy region

Jiaolong Zeng,[1,2] Gang Zhao,[1] and Jianmin Yuan[1,2]
[1]*National Astronomical Observatories, Chinese Academy of Sciences, 20A Datun Road, Chaoyang District, Beijing 100012, People's Republic of China*
[2]*Department of Applied Physics, National University of Defense Technology, Changsha 410073, People's Republic of China*
(Received 17 February 2004; published 13 August 2004)

The transmission spectrum has been calculated using a detailed-level-accounting model for iron plasmas in local thermodynamic equilibrium in the 2*p*-3*d* excitation energy region. The calculation is motivated by the large difference between the theories obtained by statistical methods such as unresolved transition array and superconfiguration transition array and the experiment reported in the literature. Detailed studies have been carried out on the effects of the width of individual lines and configuration interaction. The results show that the saturation of individual lines is evident in the transmission. These effects should be considered carefully to obtain an accurate opacity or transmission. In view of the uncertainties in the experiment, rather good agreement is found between our theoretical result and the experiment when these effects are taken into account in the calculation.

DOI: 10.1103/PhysRevE.70.027401 PACS number(s): 52.25.Os, 32.70.Jz, 32.90.+a

Absorption coefficients are crucial data in the study of inertial confinement fusion, x-ray lasers, and magnetic fusion plasmas. For iron plasmas, among other practical applications, accurate absorption coefficients are also important in astrophysics. Compared with hydrogen and helium, iron constitutes a small fraction, but its opacity plays a major role in the radiative transfer in astrophysical plasmas such as the Sun. Analysis of helioseismological data is very sensitive to the opacity of iron inside the Sun, and improvement of opacity data is important to model the Sun's oscillations. Therefore, a few experimental measurements [1–6] have been made during the past decade in order to accurately determine the radiative opacity of iron plasmas. The progress in the knowledge of iron opacity and the use of more accurate opacity have clarified a few questions in astrophysics. Chenais-Popovics [7] gave a review on the progress of the opacity measurements for astrophysics in the laboratory.

The measurements [1–6] mentioned above are limited to the photon energy region <300 eV. Chenais-Popovics *et al.* [8] extended the opacity measurement of iron plasmas to a higher photon energy region in the vicinity of 730 eV. The temperature of the plasma is around 20 eV and the areal density is $\rho L = 20\ \mu\mathrm{g/cm}^2$. The mass density is estimated to be about $0.004\ \mathrm{g/cm}^3$. Absorption of the 2*p*-3*d* transitions of Fe^{4+}–Fe^{9+} has been observed in the experiment. The authors used the supertransition array codes SCO [9] and STA [10] and detailed spin-orbit-split arrays (SOSA) calculations [11] to interpret the experimental transmission. The detailed SOSA calculation is based on the unresolved transition array (UTA) formalism developed by Bauche *et al.* [12], where all the lines of a transition array merge into one broadband. However, as the authors pointed out in their paper, the calculated absorptions are much stronger than the experiment. To obtain the measured transmission, the areal density has to be decreased by a factor of 2.7 for the SCO and STA codes and by a factor of 1.7 for SOSA calculation. The large difference between theory and experiment is beyond the experimental uncertainties caused by: the influence of the second-order spectrum, the thickness uncertainty, and the temporal and spatial inhomogeneity of the foil. As a result, Chenais-Popovics *et al.* [8] suggested that one has to investigate the effect of individual lines in detail to have a better comparison with the experiment.

To the best of our knowledge, such a detailed calculation in the 2*p*-3*d* energy region has not been carried out for Fe plasmas as of yet. In the present work, we calculate the transmission spectrum of Fe plasma under the prototype experimental condition of Chenais-Popovics *et al.* [8] using a detailed-level-accounting (DLA) treatment. It is similar to the detailed-term-accounting model applied to the aluminum plasmas [13–15], except that fine-structure energy levels and oscillator strengths are treated in the former by solving the fully relativistic Dirac equation. In this DLA model, we considered all major spectral line broadening mechanisms, including natural lifetime broadening (autoionization and radiative lifetime), electron impact, and Doppler broadening. The effects of the width of individual lines on the transmission are studied in some detail.

For a plasma of temperature T and mass density ρ in local thermodynamic equilibrium, the fraction of radiation transmitted F at photon energy $h\nu$ with respect to some incident source of arbitrary intensity is given by

$$F(h\nu) = e^{-\rho\kappa'(h\nu)L}, \tag{1}$$

where L is the path length traversed by the light source through the plasma and $\kappa'(h\nu)$ is the radiative opacity (the prime on the opacity denotes that stimulated emission has been included), which is given by

$$\rho\kappa'(h\nu) = \sum_i \left[\left(\sum_{ll'} N_{il}\sigma_{ill'}(h\nu) + \sum_l N_{il}\sigma_{il}(h\nu) \right) \right] \times (1 - e^{-h\nu/k_B T}), \tag{2}$$

where $\sigma_{ill'}(h\nu)$ is the photoexcitation cross section from level l to l' of ion i, and $\sigma_{il}(h\nu)$ is the photoionization cross section from level l of ion i. The free-free absorption and scattering are assumed to be negligible. N_{il} is the population

TABLE I. Linewidths (in meV) contributed by autoionization (Γ_a), radiative lifetime (Γ_r), electron impact (Γ_e), and Doppler (Γ_d) broadening for some strong transitions of the $3d$-$2p^{-1}3d^2$ transition array of Fe VIII. ΔE is the transition energy in eV and f_l is the length form of the oscillator strength

Transition	ΔE	f_l	Γ_a	Γ_r	Γ_e	Γ_d
$3d_{3/2}$-$[(2p_{3/2}^{-1}3d_{3/2})_2 3d_{5/2}]_{5/2}$	733.10	0.1105	148	<5	10	34
$3d_{3/2}$-$[(2p_{3/2}^{-1}3d_{3/2})_1 3d_{5/2}]_{5/2}$	735.14	0.2420	129	<5	10	34
$3d_{3/2}$-$[(2p_{3/2}^{-1}3d_{3/2})_3 3d_{5/2}]_{1/2}$	736.13	0.1320	104	<5	10	34
$3d_{3/2}$-$[(2p_{1/2}^{-1}3d_{3/2})_2 3d_{5/2}]_{5/2}$	740.51	0.1900	102	<5	10	34
$3d_{3/2}$-$[2p_{1/2}^{-1}(3d_{5/2}^2)_2]_{5/2}$	741.62	0.1275	128	<5	10	34
$3d_{3/2}$-$[2p_{1/2}^{-1}(3d_{5/2}^2)_2]_{1/2}$	745.15	0.1096	90	<5	10	35
$3d_{3/2}$-$[2p_{1/2}^{-1}(3d_{5/2}^2)_2]_{3/2}$	746.91	0.2900	133	<5	10	35
$3d_{3/2}$-$[(2p_{1/2}^{-1}3d_{3/2})_1 3d_{5/2}]_{3/2}$	747.85	0.1966	140	<5	10	35
$3d_{5/2}$-$[2p_{3/2}^{-1}(3d_{5/2}^2)_4]_{7/2}$	733.93	0.1380	109	<5	10	34
$3d_{5/2}$-$[(2p_{1/2}^{-1}3d_{3/2})_1 3d_{5/2}]_{5/2}$	745.94	0.4510	138	5	10	35
$3d_{5/2}$-$[2p_{1/2}^{-1}(3d_{5/2}^2)_2]_{3/2}$	746.66	0.1250	133	<5	10	35
$3d_{5/2}$-$[(2p_{1/2}^{-1}3d_{3/2})_1 3d_{5/2}]_{7/2}$	746.73	0.3210	195	<5	10	35
$3d_{5/2}$-$[(2p_{1/2}^{-1}3d_{3/2})_1 3d_{5/2}]_{3/2}$	747.61	0.1503	140	<5	10	35

density for level l of ion stage i obtained from the Boltzmann distribution function

$$N_{il} = g_{il}(N_i/Z_i)e^{-E_{il}/k_BT}, \tag{3}$$

where g_{il} is the statistical weight for level l of ion i, Z_i is the partition function of ion i, N_i is the population of ion i, E_{il} is the energy of level l of ion i above the ground state, and k_B is Boltzmann's constant. N_i can be obtained by solving the Saha equation [16]. The ionization potential depression is considered by using the Debye-Huckel model. The bound-bound cross section for a given level-to-level line can be expressed in terms of the oscillator strength $f_{ill'}$ as

$$\sigma_{ill'} = \frac{\pi h e^2}{m_e c} f_{ill'} S(h\nu), \tag{4}$$

where h is Planck's constant, c is the speed of light in vacuum, e is the electron charge, m_e is the electron rest mass, and S is the line-shape function, which is taken to be the Voigt profile with the major broadening mechanism being taken into account. The atomic data required in the calculations are obtained using the flexible atomic code (FAC) developed by Gu [17]. A fully relativistic approach based on the Dirac equation is used throughout the entire package.

First, let us inspect the linewidths caused by different broadening mechanisms. Under the experimental condition, Fe VIII is one of the most abundant ions in the plasma. Take the lines of transition array $(3s^23p^6)3d-2p^{-1}(3s^23p^6)3d^2$ of Fe VIII as examples. Table I shows the various linewidths [full width at half maximum (FWHM)] caused by the broadening mechanisms mentioned above. The Doppler width is connected with the temperature of the plasma and transition energy and thus it is easy to obtain. The autoionization width shown in Table I is obtained by Dirac atomic R-matrix code (DARC) [18], while electron impact broadening is obtained from the simplified semiempirical method [19]. The width of radiative lifetime can be estimated from the oscillator strengths. It can easily be seen that the autoionization width is the largest among all the broadening mechanisms for this transition array of Fe VIII, while the width of the radiative lifetime is the smallest.

In principle, in addition to the autoionization width, the detailed line profile should be considered as well because the $2p$-$3d$ excited states are autoionized ones. However, as the direct channels for both the valence excited M-shell thresholds and the inner L-shell photoionization thresholds are far away from the $2p$-$3d$ excitation energy region, the interactions between the direct and indirect photoionization channels are very weak. As a result, the line profile tends nearly to a Lorentzian profile. This has been demonstrated in the $1s$-$2p$ transitions in aluminum plasmas [13]. Thus the individual line profile is not a critical factor in opacity calculations.

As there is a large amount of transitions, the calculation of the autoionization widths is very time-consuming. From an inspection of Table I, we can see that the autoionization widths of more than 50% lines are about 140 meV. If we take the autoionization widths of all the transitions of different ionization stages to be 140 meV and if the linewidths caused by other mechanisms are calculated by the methods mentioned above, we get the calculated transmission spectrum shown in Fig. 1(a) for an iron plasma at a temperature of 20 eV and a density of 0.004 g/cm^3. This spectrum is highly resolved and shows rich spectral line structures. Note that the saturation effect is evident for some strong lines. Davidson *et al.* [20] and Chenais-Popovics *et al.* [21] studied this effect and concluded that the UTA and STA formalisms cannot correctly describe the saturation of the individual lines because they group many lines together and do not represent them individually with an accurate width.

Instrumental broadening can be taken into account by convoluting the data shown in Fig. 1(a) over a Gaussian function, with FWHM corresponding to the spectrometer resolution. Figure 1(b), solid line, shows the transmission with this effect having been considered. The dot-dashed,

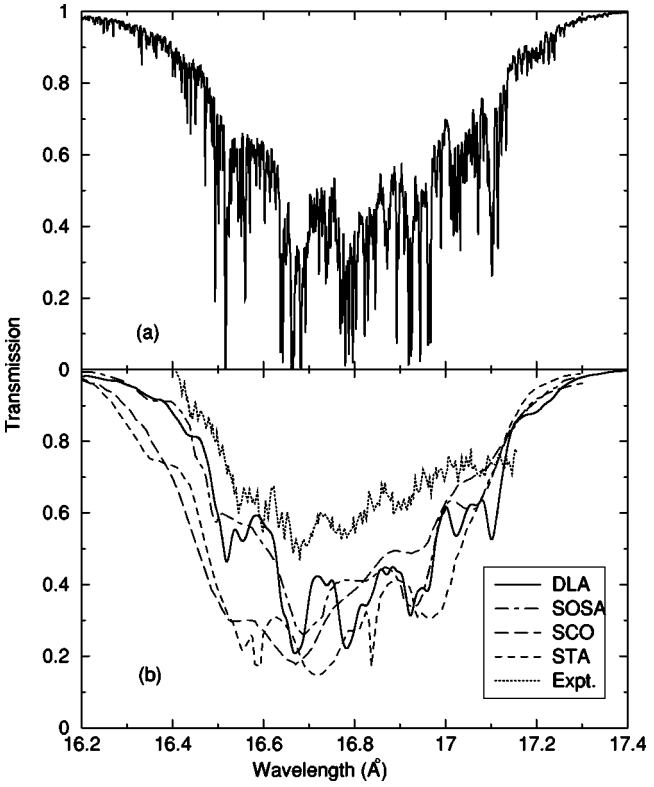

FIG. 1. Transmission calculated as a function of wavelength in Å at a temperature of 20 eV and a density of 0.004 g/cm^3. The autoionization width is taken to be 140 meV for all lines. Instrumental broadening (a) not included and (b) included.

long-dashed, and dashed lines refer to the results obtained by SOSA, SCO, and STA codes. All theories assume the iron plasma at a temperature of 20 eV and a density of 0.004 g/cm^3 except that the STA code takes a temperature of 21 eV. The dotted line in Fig. 1(b) refers to the experimental spectrum. Good agreement is observed between our calculated transmission and that of SOSA, and the two results agree best with the experiment. However, the four theoretical results which use different approximations (DLA, UTA, and STA) to treat the transitions predict stronger absorption than in the experiment.

From the viewpoint of theory, there are several factors which will affect the discrepancy between the DLA theory and experiment. First, the above calculation used an equivalent autoionization width 140 meV for all transitions. In fact, for most lines from highly excited levels, the autoionization width is much smaller than 140 meV and the typical value is about 20 meV or less. Using the autoionization widths obtained by FAC code for all transitions, the calculated transmission is shown in Fig. 2 in a solid line. To have a better understanding of the plasma condition, we have also obtained the transmission at temperatures of 18 and 22 eV. From a comparison between the theoretical and experimental transmission, one can conclude that the experimental spectrum has mixed characteristics of the three temperatures. In the short-wavelength ward, the temperature of the iron plasma should be between 18 and 20 eV from the DLA results. On the other hand, in the long-wavelength range, the

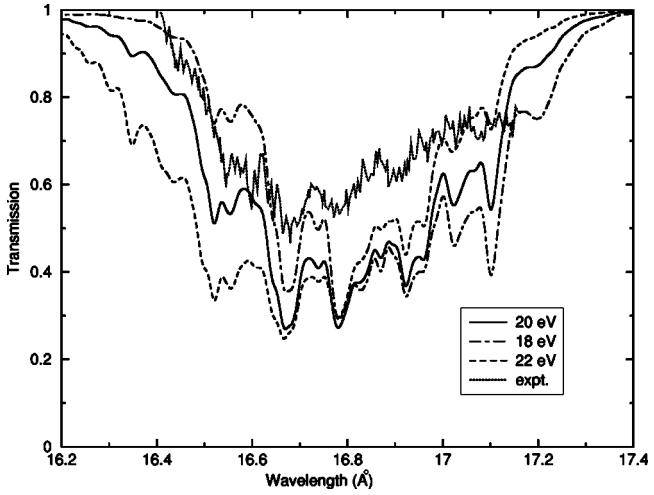

FIG. 2. Transmission at temperatures of 18, 20, and 22 eV with autoionization widths calculated by FAC for all lines.

temperature seems closer to 22 eV. Therefore, nonhomogeneity of the experimental sample and small temperature gradient existed in the experiment. At the same time, one can see that the transmission is very sensitive to the temperature, which means that it is an ideal diagnostic tool for the temperature of the plasma. The uncertainty of the temperature diagnostics obtained by theoretical predictions should be better than ±2 eV.

The second factor that affects the discrepancy comes from the accuracy of the radiative atomic data. We have carried out a large-scale configuration interaction calculation on the oscillator strengths of Fe VIII within $n<6$ configurations. Interactions are included among the following configurations: $3s^23p^63d$, $3s^x3p^y3d^z$ $(x+y+z=9,\ x=2-0,\ y=5-3)$, $3s^23p^53dnl$, $3s^23p^43d^2nl$, $3s^23p^33d^3nl$, $3s3p^63dnl$, $3s3p^53d^2nl$, $3s3p^43d^3nl$, $3p^63d^2nl$, $3p^53d^3nl$ $(n=4,5;\ l=0,1,\ldots,n-1)$, as well as all those which can give rise to $2p$-nd and $2p$-ns transitions from the above configurations, i.e., $2p^53s^23p^63d^2$, $2p^53s^x3p^y3d^{z+1}$, etc. The results show that the effect of configuration interaction can generally lower the oscillator strengths by about 20%. Figure 3, solid line, shows the transmission at a temperature of 19 eV after this effect has been included. The dot-dashed line refers to the result obtained by SOSA with individual lines at a temperature of 20 eV and a density of 0.004 g/cm^3. Better agreement is found between both theories of DLA and SOSA with individual lines and the experiment. However, Chenais-Popovics *et al.* [8] pointed out that the effect of second order reflected by the crystal used in their experiment is estimated to lower the experimental data by 20%. The dashed line in Fig. 3 shows the result by lowering the transmission by 20%. After taking account of the second-order effect, the agreement is good between the theory and experiment considering the experimental uncertainties mentioned above, such as nonhomogeneity of the experimental sample and temperature gradient. From a comparison of Figs. 2 and 3, one can see that the effect of configuration interaction plays a more important role than that of linewidth. No shift is made for the line positions in all our results. Besides good agreement for the overall transmission, very good agreement is also found

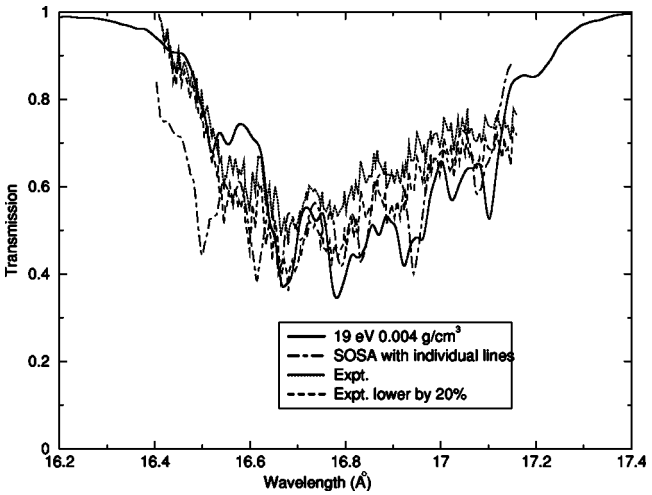

FIG. 3. Transmission at a temperature of 19 eV obtained by further considering the configuration interaction effect. The dot-dashed line refers to the result obtained by SOSA with individual lines [8].

between the experimental and theoretical line positions. This is an indication of the accuracy of the present calculations. Lastly, the autoionization states may affect the remaining discrepancy. Because of the complex electron structure, there is a large amount of autoionization states for these iron ions. In the present work, we did not take into account their contributions to the partition functions. In a strict treatment, one should consider this effect.

In conclusion, the transmission spectrum has been calculated for an iron plasma using the detailed-level-accounting model. The effect of the width of individual lines has been studied in detail. The results show that the saturation of the individual lines is evident and important in the detailed transmission calculations. To obtain accurate opacity or transmission, one has to take into account the effect of the width of individual lines caused by all major broadening mechanisms in the plasmas. Considering the experimental uncertainties, reasonably good agreement is obtained between theory and experiment after the linewidth effect and configuration interaction effect have been considered in the calculations. Further experimental and theoretical studies are needed to clarify the remaining difference between experiment and theory.

This work was supported by the National Science Fund for Distinguished Young Scholars under Grant No. 10025416, the National Natural Science Foundation of China under Grant No. 10204024, No. 10373014, and No. 19974075, the National High-Tech ICF Committee in China, and China Research Association of Atomic and Molecular Data.

[1] L. B. DaSilva *et al.*, Phys. Rev. Lett. **69**, 438 (1992).
[2] G. Winhart *et al.*, J. Quant. Spectrosc. Radiat. Transf. **54**, 437 (1995).
[3] G. Winhart *et al.*, Phys. Rev. E **53**, R1332 (1996).
[4] P. T. Springer *et al.*, Phys. Rev. Lett. **69**, 3735 (1992).
[5] P. T. Springer *et al.*, J. Quant. Spectrosc. Radiat. Transf. **51**, 371 (1994).
[6] P. T. Springer *et al.*, J. Quant. Spectrosc. Radiat. Transf. **58**, 927 (1997).
[7] C. Chenais-Popovics, Laser Part. Beams **20**, 291 (2002).
[8] C. Chenais-Popovics *et al.*, Astrophys. J., Suppl. Ser. **127**, 275 (2000).
[9] T. Blenski, A. Grimaldi, and F. Perrot, Phys. Rev. E **55**, R4889 (1997).
[10] A. Bar-Shalom *et al.*, Phys. Rev. A **40**, 3183 (1989).
[11] C. Bauche-Arnoult, J. Bauche, and M. Klapisch, Phys. Rev. A **31**, 2248 (1985).
[12] J. Bauche, C. Bauche-Arnoult, and M. Klapisch, Adv. At. Mol. Phys. **23**, 131 (1987).
[13] Jiaolong Zeng, Fengtao Jin, Jianmin Yuan, and Qisheng Lu, Phys. Rev. E **62**, 7251 (2000).
[14] Jiaolong Zeng, Jianmin Yuan, and Qisheng Lu, Phys. Rev. E **64**, 066412 (2001).
[15] Jiaolong Zeng and Jianmin Yuan, Phys. Rev. E **66**, 016401 (2002).
[16] R. D. Cowan, *Theory of Atomic Spectra* (University of California Press, Berkeley, 1981).
[17] M. F. Gu, Astrophys. J. **582**, 1241 (2003).
[18] P. H. Norrington and I. P. Grant, J. Phys. B **20**, 4869 (1987).
[19] M. S. Dimitrijevic and N. Konjevic, Astron. Astrophys. **172**, 345 (1987).
[20] S. J. Davidson *et al.*, in *Laser Interaction with Matter Proceedings*, edited by G. Velarde, E. Minguez, and J. M. Perlado (World Scientific, Singapore, 1989), pp. 163–166.
[21] C. Chenais-Popovics *et al.*, Phys. Rev. A **40**, 3194 (1989).